Virulence 4:8, 686–697; November 15, 2013; © 2013 Landes Bioscience

Cerebral tissue oxygenation impairment during experimental cerebral malaria

Pedro Cabrales[1,2,*], Yuri C Martins[1], Peng Kai Ong[1], Graziela M Zanini[1,3], John A Frangos[1], and Leonardo JM Carvalho[1,4]

[1]Center for Malaria Research; La Jolla Bioengineering Institute; San Diego, CA USA; [2]Department of Bioengineering; University of California; San Diego, CA USA; [3]Parasitology Service; Evandro Chagas Clinical Research Institute; Fiocruz; Rio de Janeiro, Brazil; [4]Laboratory of Malaria Research; Oswaldo Cruz Institute; Fiocruz; Rio de Janeiro, Brazil

Keywords: cerebral malaria, pial microcirculation, oxygen tension, oxygen delivery, anemia

Ischemia and hypoxia have been implicated in cerebral malaria (CM) pathogenesis, although direct measurements of hypoxia have not been conducted. C57BL/6 mice infected with *Plasmodium berghei* ANKA (PbA) develop a neurological syndrome known as experimental cerebral malaria (ECM), whereas BALB/c mice are resistant to ECM. In this study, intravital microscopy methods were used to quantify hemodynamic changes, vascular/tissue oxygen (O_2) tension (PO_2), and perivascular pH in vivo in ECM and non-ECM models, employing a closed cranial window model. ECM mice on day 6 of infection showed marked decreases in pial blood flow, vascular (arteriolar, venular), and perivascular PO_2, perivascular pH, and systemic hemoglobin levels. Changes were more dramatic in mice with late-stage ECM compared with mice with early-stage ECM. These changes led to drastic decreases in O_2 delivery to the brain tissue. In addition, ECM animals required a greater PO_2 gradient to extract the same amount of O_2 compared with non-infected animals, as the pial tissues extract O_2 from the steepest portion of the blood O_2 equilibrium curve. ECM animals also showed increased leukocyte adherence in postcapillary venules, and the intensity of adhesion was inversely correlated with blood flow and O_2 extraction. PbA-infected BALB/c mice displayed no neurological signs on day 6 and while they did show changes similar to those observed in C57BL/6 mice (decreased pial blood flow, vascular/tissue PO_2, perivascular pH, hemoglobin levels), non-ECM animals preserved superior perfusion and oxygenation compared with ECM animals at similar anemia and parasitemia levels, resulting in better O_2 delivery and O_2 extraction by the brain tissue. In conclusion, direct quantitative assessment of pial hemodynamics and oxygenation in vivo revealed that ECM is associated with severe progressive brain tissue hypoxia and acidosis.

Introduction

Cerebral malaria (CM) is a potentially lethal complication of *Plasmodium falciparum* infections that mainly affects children in areas of high malaria endemicity.[1] CM is characterized by coma in patients with asexual blood stage parasitemia in the absence of other identifiable causes of encephalopathy. CM is commonly associated with other complications such as severe anemia and metabolic acidosis.[1-3] Indeed, acidosis has been shown to be markedly related to increased mortality in CM patients.[4] While the pathogenesis of CM has not been elucidated, it is likely to be multi-factorial, involving parasite sequestration, reduced microcirculatory blood flow, inflammatory responses, and breakdown of the blood–brain barrier.[1,5] Postmortem studies in CM patients revealed parasitized red blood cell (pRBC) aggregates sequestered in inflamed endothelium of blood brain vessels, and in vivo analysis of retinal blood vessels showed impaired perfusion and vascular obstructions.[6,7] Impairments of cerebral microcirculatory blood flow are thought to cause an ischemic process leading to cerebral hypoxia which, if sustained, can be fatal or, if reversed by treatment, can still lead to neurological sequelae.[8] Examination of blood flow, oxygen (O_2) tensions, and O_2 transport at the level of individual vessels is essential to establish the relation between hemodynamic and oxidative conditions associated with pathophysiological manifestations of CM.

Cerebral hypoxia in human CM has not been directly assessed due to limitations in methods for determining cerebral O_2 levels in comatose patients. Observations like vascular occlusion, increased lactate levels in the cerebrospinal fluid, and retinal whitening (hypoperfusion) provide indirect indications that CM involves limitations in brain oxygenation.[9-11] Similarly, cerebral hypoxia during experimental (murine) cerebral malaria (ECM) by *Plasmodium berghei* ANKA has been suggested based on lactate accumulation, expression of hypoxia-inducible factor-1α (HIF-1α), and positive staining by the hypoxia probe (pimonidazole).[12-14] These findings suggest changes in energy metabolism, activation of transcription factors, and bioreductive conditions during ECM; however, they do not provide direct information about O_2 tensions (PO_2s). Therefore, direct

*Correspondence to: Pedro Cabrales; Email: pcabrales@ucsd.edu
Submitted: 07/11/2013; Revised: 08/26/2013; Accepted: 09/03/2013
http://dx.doi.org/10.4161/viru.26348

Table 1. C57BL/6 (ECM-susceptible) and BALB/c (ECM-resistant) mice

A. Blood O_2 transport characteristics, perivascular pH, and core					
Group	**Hematocrit %**	**Hb g/d**	**Perivascular pH**	**p50 mmHg**	**Temperature °C**
C57BL/6	49 ± 1	15.4 ± 0.4	7.250 ± 0.012	43 ± 2	38.1 ± 0.5
BALB/c	48 ± 2	15.0 ± 0.5	7.272 ± 0.024	42 ± 1	37.8 ± 0.3

B. Pial microcirculation hemodynamics and oxygen tensions						
Group			***n***	**Bloodflow nL/s**	**PO_2 mmHg**	**O_2 Sat %**
C57BL/6	Arterioles	Small (20–40 μm)	7	4.3 ± 1.5	–	–
		Mid (40–60 μm)	32	7.2 ± 2.7	53.1 ± 2.1	66.7 ± 2.6
		Large (60–80 μm)	12	10.2 ± 2.0	–	–
	Venules	Small (20–40 μm)	11	1.9 ± 1.1	–	–
		Mid (40–60 μm)	43	4.1 ± 1.6	30.3 ± 2.1	26.3 ± 2.4
		Large (60–80 μm)	16	6.2 ± 1.6	–	–
BALB/c	Arterioles	Small (20–40 μm)	5	3.9 ± 1.4	–	–
		Mid (40–60 μm)	30	6.5 ± 1.8	51.3 ± 2.9	64.8 ± 3.8
		Large (60–80 μm)	8	13.8 ± 1.4[a]	–	–
	Venules	Small (20–40 μm)	9	1.8 ± 1.2	–	–
		Mid (40–60 μm)	34	3.9 ± 1.8	33.1 ± 3.0	30.1 ± 3.4
		Large (60–80 μm)	11	5.8 ± 2.1	–	–

Values are means ± SD. [a]$P < 0.05$ compared with C57BL/6. Hb, hemoglobin; P50, PO_2 at which 50% of the Hb is saturated with O_2.

assessments of PO_2s in cerebral vessels in vivo during ECM are missing, especially in relation to hemodynamic and inflammatory changes.

Optical techniques provide valuable information for the study of hemodynamics and O_2 tension.[15] Intravital microscopy of the closed cranial window transcends brain histochemical analyses, allowing the visualization and quantification of the dynamic events of pial microcirculation.[16] This technique is an important tool in determining the underlying pathological features contributing to ECM progression.[17-19] The pial microcirculation shares the same general behavior and functionality of the brain circulation, including the blood–brain barrier properties.[20] During ECM, pial vessels show pathology similar to that observed in parenchymal vessels, such as leukocyte adhesion, vascular occlusion, hypoperfusion, leakage, and microhemorrhages.[18] Lastly, the pial arterioles "dive" into the brain parenchyma to nourish it, and pial venules emerge from the parenchyma.[20] Therefore, the O_2 extraction of the brain tissues receiving blood flow from pial vessels can be estimated by the difference in O_2 transported by pial arterioles and venules.[21]

Monitoring hemodynamics and inflammatory changes within the pial microcirculation during the course of malaria infection in mice has shown that ECM pathogenesis is associated with microcirculatory complications including decreased blood flow, vasoconstriction, vascular plugging by adherent cells, and microhemorrhages.[17-19] The present study analyzes the pial microenvironment during pathophysiological conditions resulting from *Plasmodium berghei* ANKA (PbA) infection in C57BL/6 mice, which are prone to ECM development, compared with PbA infection in BALB/c mice, which are resistant to ECM development.[22,23] Phosphorescence quenching microscopy (PQM) was used to measure O_2 tensions and pH-sensitive fluorescence was used to determine perivascular tissue pH.[24] Since vascular occlusion is thought to be the major contributor to hypoperfusion and hypoxia in CM, we studied the role of leukocyte attachment to endothelium in relation to changes in flow and oxygenation.

Results

Normal physiological ranges for the measured variables

Table 1 presents the summary of blood parameters, microvascular diameters, blood flows, and O_2 tensions for control C57BL/6 and BALB/c mice. These data were generated because no previously reported values for cerebral PO_2 distribution and hemodynamic parameters were available using the close cranial window and PQM.

Systemic and pial microenvironment physiological characteristics of C57BL/6 and BALB/c mice

Control animals showed normal hematocrit, hemoglobin, blood P50 (the partial pressure of O_2 required to saturate 50% of Hb), core body temperature and perivascular pH (7.250 ± 0.012 for C57BL/6 and 7.272 ± 0.024 for BALB/c) as presented in **Table 1A**.

Pial microcirculation hemodynamics

Blood flow in small arterioles and venules (20 to 40 μm) or mid-size arterioles and venules (40 to 60 μm) for control C57BL/6 and BALB/c mice were not different (**Table 1B**). Only blood flow in large arterioles (60 to 80 μm) was higher for control BALB/c mice compared with control C57BL/6 mice.

Table 2. Infected C57BL/6 (ECM-susceptible) and BALB/c (ECM-resistant) mice: Blood O_2 transport characteristics, perivascular pH, and core temperature

Group		Hematocrit %	Hb g/d	Perivascular pH	P50 mmHg	Parasitemia %	Temperature °C
C57BL/6	Uninfected	48 ± 2	15.0 ± 0.6	7.247 ± 0.007	42 ± 1	–	38.2 ± 0.4
	Infected	29 ± 4[a]	8.4 ± 0.8[a]	7.103 ± 0.014[a]	46 ± 2[a]	11.2 ± 4.7[a]	34.2 ± 2.7[a]
BALB/c	Uninfected	49 ± 1	15.2 ± 0.4	7.263 ± 0.014	42 ± 1	–	37.73 ± 0.3
	Infected	33 ± 2	9.7 ± 0.5[a]	7.197 ± 0.012[a,b]	44 ± 1[a]	10.6 ± 2.4[a]	35.8 ± 0.7[a,b]

Values are means ± SD. Hb, hemoglobin, P50, PO_2 at which 50% of the Hb in the blood are saturated with O_2. [a]$P < 0.05$ compared with their uninfected control; [b]$P < 0.05$ compared with infected C57BL/6.

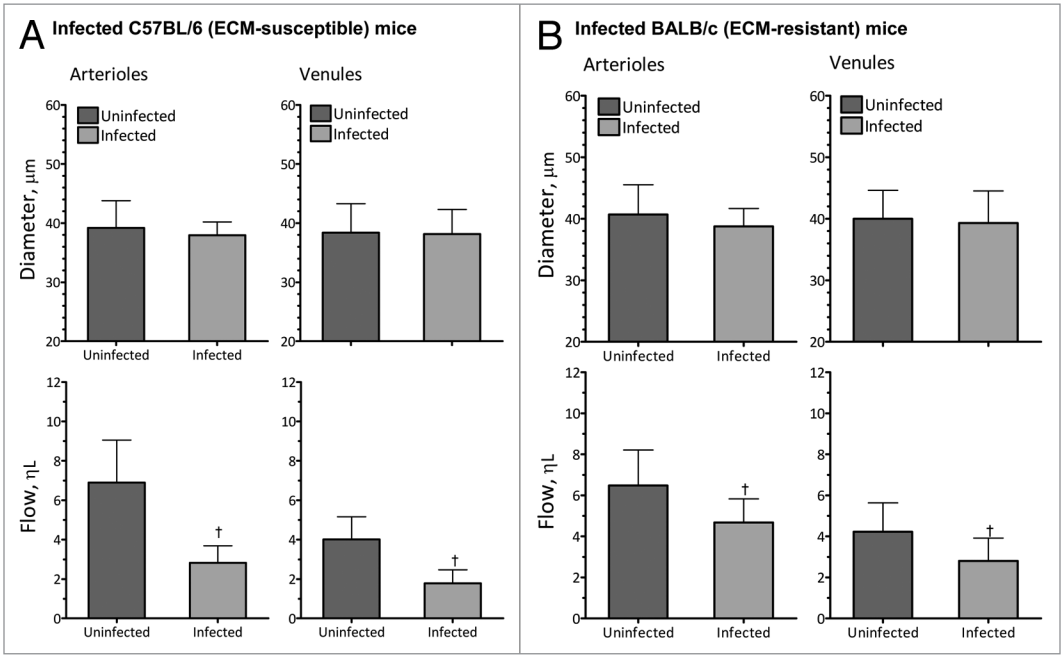

Figure 1. Arteriolar, venular and perivascular PO_2s effects of PbA infection in ECM (C57BL/6) and Non-ECM (BALB/c) models. (**A**) PbA infected C57BL/6 (ECM susceptible). (**B**) PbA infected BALB/c (ECM resistant). †$P < 0.05$ compared with uninfected control. Data presented includes arterioles and venules comparable in size (30 to 50 µm). The studied vasculature was not different in diameter for arterioles or venules between groups. A total of 68 arterioles and 77 venules were analyzed in the C57BL/6 infected group, and 46 arterioles and 58 venules were analyzed in the C57BL/6 uninfected group. Additionally, 52 arterioles and 62 venules were analyzed in the BALB/c infected group, and 35 arterioles and 47 venules were analyzed in the BALB/c uninfected group. Marked decreases in arteriolar and venular blood flows to 41% and 44%, respectively, of the blood flows of uninfected mice were measured in C57BL/6 infected mice. Infected BALB/c mice also exhibited decrease in arteriolar and venular blood flows to 67% and 62%, respectively, of the blood flows of uninfected BALB/c mice.

Pial oxygen tensions

PO_2s and O_2 saturations of midsize arterioles and venules (40 to 60 µm) of uninfected animals were not different between C57BL/6 and BALB/c mice (**Table 1B**). Similarly, tissue (perivascular) PO_2s were not different between C57BL/6 (31.6 ± 1.0 mmHg) and BALB/c (32.5 ± 2.3 mmHg) mice. Calculated O_2 delivery was not different between uninfected C57BL/6 and BALB/c. Calculated O_2 extraction was 9% lower in uninfected BALB/c compared with uninfected C57BL/6, although no statistical significance was reached. Consequently, O_2 extraction ratio was lower for uninfected BALB/c compared with uninfected C57BL/6.

PbA infection in C57BL/6 (ECM-susceptible) and BALB/c (ECM-resistant) mice

On day 6 of infection, PbA-infected C57BL/6 and BALB/c mice showed similar levels of parasitemia and significant decreases in hematocrit and hemoglobin levels compared with the uninfected groups ($P < 0.05$). **Table 2** presents hematocrit, hemoglobin, blood P50, and core temperature for all the groups. Perivascular pH was decreased in both infected groups, although the perivascular pH of the BALB/c infected was significantly higher than the C57BL/6 infected group. The C57BL/6 infected group showed hypothermia, with core body temperature decreased to 34.2 ± 2.7 °C in the infected group, compared with 38.2 ± 0.4 °C in the uninfected group ($P < 0.05$). The BALB/c infected group showed hypothermia compared with the uninfected group ($P < 0.05$) as well, though the temperature of the BALB/c infected was significantly higher than the C57BL/6 infected. Blood P50s were measured at interstitial pH and core body temperature. C57BL/6 and BALB/c infected animals showed significant decreases in blood O_2 affinities, with blood P50 significantly higher compared with their uninfected controls ($P < 0.05$).

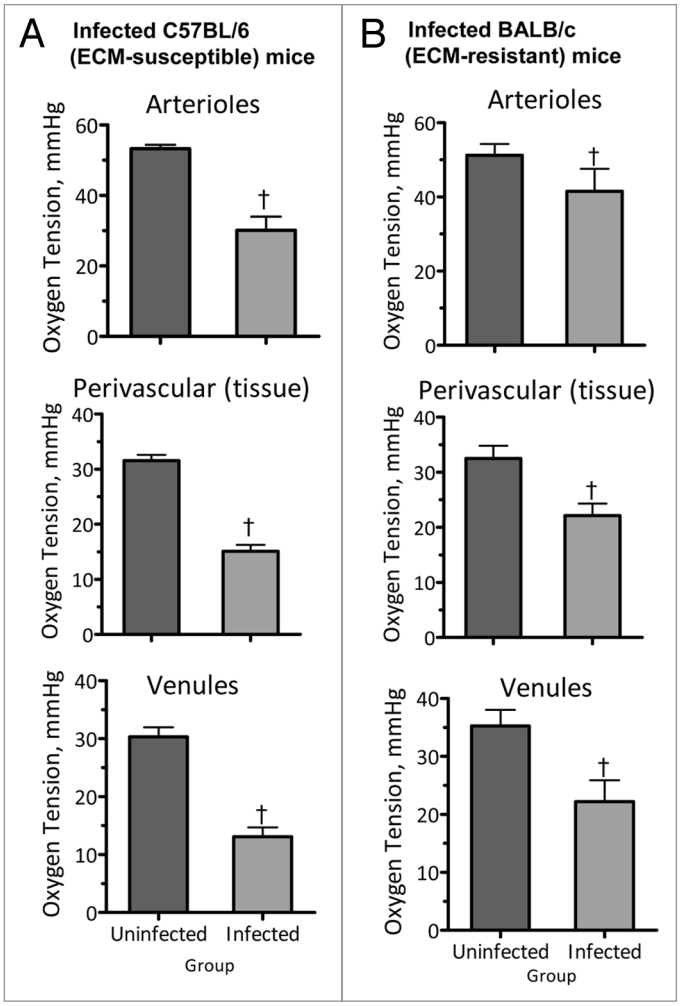

Figure 2. Arteriolar, venular, and perivascular PO_2s effects of PbA infection in ECM (C57BL/6) and Non-ECM (BALB/c) models. (**A**) PbA infected C57BL/6 (ECM model). (**B**) PbA infected BALB/c (non-ECM model). †$P < 0.05$ compared with uninfected control. The arteriolar PO_2 of infected C57BL/6 mice was 56% of the arteriolar PO_2 of uninfected ECM animals, thus the arteriolar SO_2 (O_2 saturation) of infected C57BL/6 mice was 34% of the arteriolar SO_2 of the uninfected C57BL/6 mice. The perivascular tissue PO_2 of the C57BL/6 and BALB/c infected groups was 47% and 68% of the perivascular tissues PO_2 of their uninfected controls, respectively.

Hemodynamic effects of PbA infection in C57BL/6 (ECM-susceptible) and BALB/c (ECM-resistant) mice

Complete hemodynamics data for arterioles and venules comparable in size (30 to 50 μm) are presented in **Figure 1**. Marked decreases in arteriolar and venular blood flows were observed in both infected groups compared with their uninfected controls ($P < 0.05$). However, the arteriolar and venular blood flows of ECM-susceptible C57BL/6 mice decreased to 41% and 44%, respectively, of the blood flows of uninfected mice, whereas the bloodflows of ECM-resistant BALB/c mice decrease to 67% and 62%, respectively.

Arteriolar, venular, and perivascular PO_2s effects of PbA infection in C57BL/6 (ECM-susceptible) and BALB/c (ECM-resistant) mice

Arteriolar, venular, and perivascular PO_2s for both C57BL/6 and BALB/c infected mice were significantly lower than their uninfected controls ($P < 0.05$). Again, the changes were more drastic in ECM-susceptible C57BL/6 mice than in ECM-resistant BALB/c mice (**Fig. 2**). The arteriolar SO_2 of C57BL/6 and BALB/c infected groups was 34% and 72% of the arteriolar SO_2 of their uninfected controls, and the venular SO_2 of C57BL/6 and BALB/c infected groups was 10% and 46% of the venular SO_2 of their uninfected controls, respectively. C57BL/6 and BALB/c infected groups presented lower perivascular PO_2s compared with their uninfected controls.

Perivascular pH effects of PbA infection in C57BL/6 (ECM-susceptible) and BALB/c (ECM-resistant) mice

C57BL/6 and BALB/c infected groups had significantly lower pH compared with their uninfected controls (**Table 1**). Perivascular pH of the BALB/c infected groups was significantly higher than the C57BL/6 infected group ($P < 0.05$).

Oxygen delivery and extraction changes due to PbA infection in C57BL/6 (ECM-susceptible) and BALB/c (ECM-resistant) mice

C57BL/6 and BALB/c infected groups had lower O_2 delivery and extraction compared with their uninfected controls (**Fig. 3**). O_2 delivery in the infected C57BL/6 mice was only 11% of that in the uninfected control, whereas O_2 delivery for the infected BALB/c mice was 37% of that in the uninfected control. Similarly, O_2 extraction in the infected C5BL/6 mice was only 13% of that in the uninfected control, whereas O_2 extraction in the infected BALB/c mice was 48% of that in the uninfected control. The relationship between O_2 delivery and O_2 extraction can be summarized using the O_2 extraction ratio, which describes the capacity to compensate for changes in O_2 supply and consumption. Increases in O_2 extraction ratio are associated with an inability to maintain baseline O_2 consumption, leading to metabolic acidosis, hemodynamic instability, and eventual death. The O_2 extraction ratio in the infected C57BL/6 mice was 92%, compared with the O_2 extraction ratio of 79% in their uninfected control. The O_2 extraction ratio in the infected BALB/c mice increased to 88%, compared with the O_2 extraction ratio of 70% in their uninfected control. The O_2 extraction ratios are higher for than C57BL/6 mice than the BALB/c mice, demonstrating the more drastic inability to maintain O_2 consumption among the former than the latter.

Oxygen transport differences between PbA infection in C57BL/6 (ECM-susceptible) and BALB/c (ECM-resistant) mice

Blood O_2 transport characteristics were studied using the blood O_2 equilibrium curves for C57BL/6 and BALB/c infected groups and their uninfected controls (**Fig. 4**). The O_2 content takes into account O_2 saturations and O_2 carrying capacity, and the O_2 delivery takes into account O_2 content and hemodynamic changes. The highlighted ranges in **Figure 4** illustrate the zone (based on the intravascular PO_2) where each group accomplishes its O_2 exchange. In both murine models, PbA infection affected the blood O_2 equilibrium curves, decreased the O_2 carrying capacity and blood flow, worsening O_2 delivery. The pial tissues of C57BL/6 and BALB/c uninfected groups extracted their O_2 within the steepest zone of the O_2 equilibrium curve. On the other hand, the pial tissue of PbA-infected C57BL/6 mice

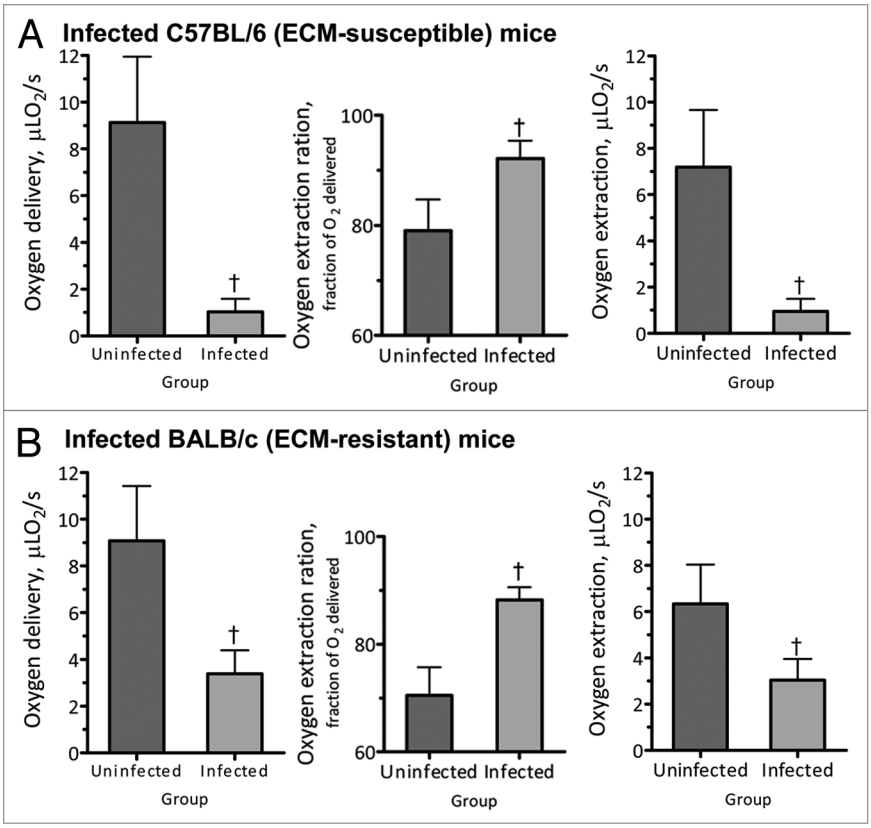

Figure 3. Oxygen delivery and extraction changes due to PbA infection in ECM (C57BL/6) and Non-ECM (BALB/c) models. (**A**) PbA-infected C57BL/6 (ECM model). (**B**) PbA-infected BALB/c (non-ECM model). †$P < 0.05$ compared with uninfected control. Calculated O_2 delivery, extraction and extraction were generated based on hemodynamic and Hb O_2 saturations. The O_2 delivery infected C57BL/6 and BALB/c group was a small fraction of the O_2 delivery of their uninfected control groups. The O_2 extraction ratio was significantly higher for the C57BL/6 and BALB/c infected animals compared with their uninfected controls.

obtained O_2 from the lower section of the blood O_2 equilibrium curve. Therefore, PbA-infection induced changes (anemia and hypoperfusion) that reduced oxygenation, especially in ECM-susceptible C57BL/6 mice, which were more sensitive to these changes than ECM-resistant BALB/c.

PbA-infected C57BL/6 mice with early- or late-stage ECM

We analyzed the hemodynamic and blood O_2 transport properties in two sub-groups of PbA-infected C57BL/6 mice on day 6 of infection, those with early-stage (moderate drops in body temperature: >34 °C, <36 °C) and those with late-stage ECM (marked drops in body temperature: <33 °C) (**Table 3**). At the time of measurements, 50% of the animals presented early signs of ECM. Early-stage ECM animals showed higher hematocrit, hemoglobin levels, and perivascular pH compared with late-stage ECM animals. Blood P50 was lower for early-stage ECM compared with late-stage ECM animals. However, parasitemia was not significantly different between the late ECM and early-stage ECM groups. In the late-stage ECM animals, the decrease in blood flow was accompanied with partial vascular network collapse. Blood flow in late-stage ECM group was significantly lower than in early-stage ECM (**Fig. 5A**). In addition, arteriolar, venular, and perivascular PO_2s were significantly lower in late-stage than in early-stage ECM mice (**Fig. 5B**). These data indicate that the clinical manifestation of late-stage ECM is associated with a severe decrease in O_2 delivery. The animals with late-stage ECM suffered a 50% reduction in O_2 carrying capacity compared with uninfected animals, but their O_2 delivery was only 7% of the uninfected animals. This corresponds to a 7-fold decrease in O_2 supply relative to the decrease in O_2 carrying capacity. The late-stage ECM animals also had lower perivascular pH compared with early-stage ECM animals ($P < 0.05$).

Adherent leukocytes in relation to blood flow and O_2 extraction in PbA-infected C57BL/6 animals with early- or late-stage ECM

There was no difference in the number of endothelium-adherent leukocytes in animals with either early- (11.0 ± 3.3 leukocytes per 100 μm) or late- (11.8 ± 2.6 leukocytes per 100 μm) stage ECM (**Fig. 6A**). In both early- and late-stage ECM cohorts, blood flow decreased as the number of adhered leukocytes increased. At comparable levels of leukocyte adhesion, however, mice with early-stage ECM showed higher blood flows than mice with late-stage ECM (**Fig. 6B**). The early-stage ECM cohort presented higher O_2 extraction compared with the late-stage ECM cohort, and in both cohorts the O_2 extraction decreased as the number of adherent leukocytes increased. The O_2 extractions for PbA-infected C57BL/6 mice for early- or late-stage ECM were different, although the numbers of adhered leucocytes were not. Therefore, O_2 extraction, per se, appears to determine the stage of ECM.

Discussion

The principal finding of this study is that the pial microvascular hemodynamics and oxygenation were drastically compromised during PbA infection in C57BL/6 mice with ECM. The pial microcirculation of ECM-resistant BALB/c mice was also affected by PbA infection, but preserved superior perfusion and oxygenation compared with ECM animals at similar anemia and parasitemia levels, resulting in better O_2 delivery and O_2 extraction by the brain tissue. The severity of the dysfunctions increased from early-state to late-stage ECM. PbA infection reduced blood flow, blood O_2 transport characteristics, and O_2 delivery that limited oxygenation in ECM mice. This study, for the first time, provides quantitative information of the changes in PO_2s and O_2 transport during ECM; it also links the underlying pathological features of ECM with O_2 delivery and extraction limitations. The pial tissue was near the hypoxic threshold in late-stage ECM, as experimental studies indicate

that the white matter has a PO_2 aerobic threshold of 5 mmHg and below this threshold cells die and the organism stays at a vegetative state.[25] This is suggested in previous studies by the accumulation of hypoxia markers, including lactate, alanine, and glutamate during ECM.[13] However, a previous study has shown that brain NAD/NADH ratio remains unchanged in ECM mice, suggesting that ECM animals did not cross the anaerobic threshold.[12] Therefore, PbA infection in the ECM model causes insufficient O_2 delivery, which in part can be a component of the neurological problems associated with CM.

The blood O_2 equilibrium curve of ECM mice reveals the key to understand the sensitivity of the pial tissue to changes in blood flow and arterial PO_2. Our blood O_2 equilibrium curves are more reliable than previous attempts, since the Bohr Effect and hypothermia were taken into account.[26] The relation between hemodynamics and PO_2 for the pial tissues showed a strong susceptibility to changes in blood flow and arteriolar PO_2, affecting O_2 delivery and limiting O_2 extraction. This is because the pial tissue extracts O_2 from the blood within the steepest zone of the blood O_2 equilibrium curve. This is not a problem in normal conditions, since the blood O_2 supplied exceeds the pial tissue's energetic demand.[27] Accordingly, PbA-infected ECM animals (C57BL/6) required a greater PO_2 gradient to extract the same amount of O_2. Thus, ECM animals may be more sensitive to changes in blood flow, since a longer RBC transit time in the pial vessels allows for more O_2 to diffuse into the hypoxic tissues, depleting the O_2 transported downstream. Reduced cerebral oxygen transport has also been described in patients with CM.[28]

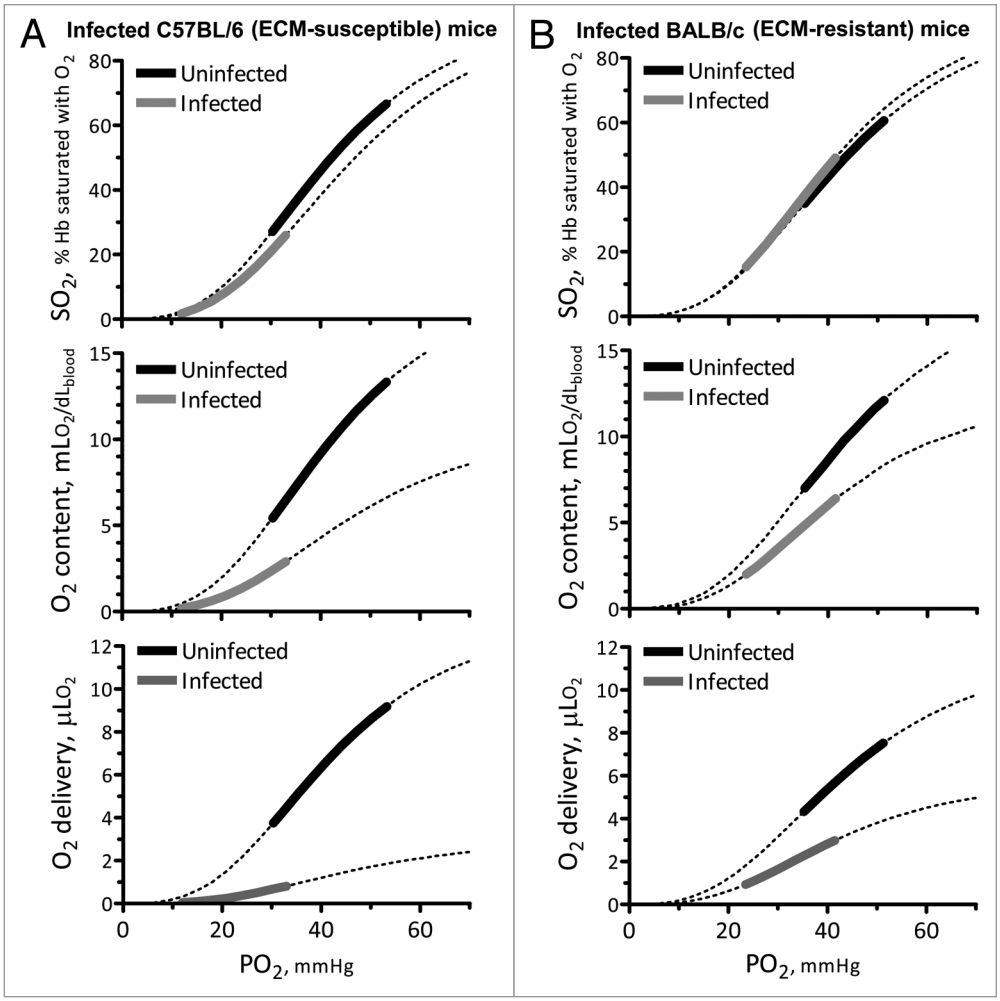

Figure 4. Oxygen transport differences between PbA infection in ECM (C57BL/6) and Non-ECM (BALB/c) models. (**A**) PbA-infected C57BL/6 (ECM model). (**B**) PbA infected BALB/c (non-ECM model). $^{\dagger}P < 0.05$ compared with uninfected control. O_2 saturation (SO_2), O_2 content and microcirculation O_2 delivery. The infected animals groups include the early-stage of ECM and late-stage of ECM. Perivascular pH and body temperature were taken into account during blood O_2 equilibrium measurements. The pial tissues of uninfected C57BL/6 and BALB/c extract O_2 within the steepest zone of the blood O_2 equilibrium curve. Therefore, the hypoperfusion and reduction in arterial PO_2 limited O_2 supply to pial tissues in the ECM model.

PbA-infected ECM and non-ECM animal models showed lower intravascular and perivascular PO_2s than animals at similar anemic level without PbA infection.[29] Anemia lowers blood viscosity and decreases vascular resistance, thus increasing blood flow;[29] although PbA infection produces anemia, in ECM-susceptible C57BL/6 but not in ECM-resistant BALB/c mice it also induces hypoperfusion resulting from increased vascular resistance downstream due to cell adhesion to the endothelium and also due to vasoconstriction.[17,18] Analysis of O_2 delivery as

Table 3. Blood O_2 transport characteristics, perivascular pH, and core temperature

Group (C57BL/6)	Hematocrit %	Hb g/d	Perivascular pH	P50[b] mmHg	Parasitemia %	Temperature °C
Early stage ECM	31 ± 3	9.4 ± 0.5	7.211 ± 0.011	44 ± 1	10.1 ± 3.5	35.3 ± 0.06
Late stage ECM	27 ± 2[a]	7.5 ± 0.6[a]	6.997 ± 0.009[a]	47 ± 2[a]	12.3 ± 3.2	32.8 ± 2.3[a]

Values are means ± SD. Hb, hemoglobin; P50, the PO_2 at which the hemoglobin becomes 50% saturated with O_2. [a]$P < 0.05$ compared with infected early stage ECM; [b]Measured at perivascular pH.

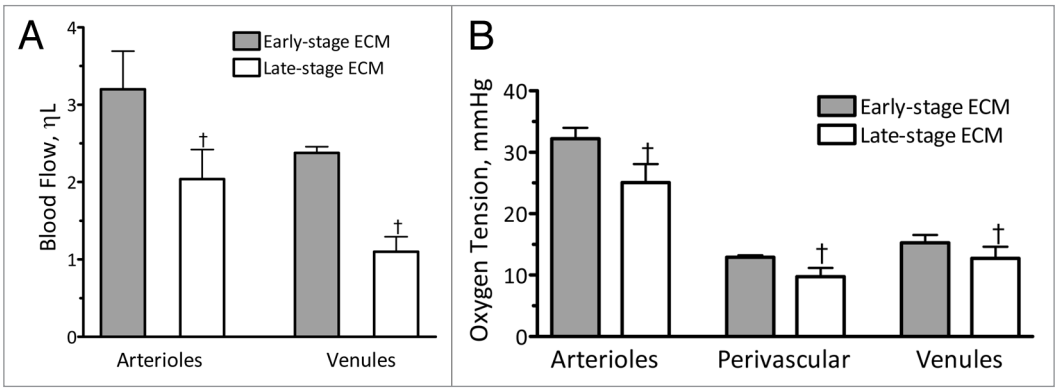

Figure 5. PbA-infected animals with early- or late-stage ECM (C57BL/6). (**A**) Microhemodynamics in ECM animals. (**B**) Oxygen tension in ECM animals. 50% of the animals in the infected group presented early-stage ECM. Animals presenting late clinical signs of ECM had significantly lower blood flows. The observed decreases in blood flow were due to low RBC velocities since blood vessels diameters were selected within a similar range (30–50 um). The arteriolar PO_2 of the animals with clinical signs of late ECM was 53% of the uninfected animals. Arteriolar, venular, and perivascular PO_2 between the early ECM and late ECM infected animals were statistically different ($P < 0.05$). These data indicate that the clinical manifestation of early-stage of ECM is associated with severe decrease in O_2 delivery.

a function of the arteriolar blood flow in normal conditions indicates that O_2 delivery is correlated with arteriolar blood flow (Spearman $R = 0.94$), and that this correlation is preserved in infected animals (Spearman $R = 0.89$). However, at late-stage ECM, there was no correlation between O_2 delivery and arteriolar blood flow, as blood arrived to the pial tissue already depleted of O_2 (SO_2 below 30%). Oxygenation changes during PbA infection were similar to the changes in oxygenation during acute brain trauma with acute anemia, as the calculated O_2 extraction tends to be progressively decreased depending on the extent of anemia, which is consistent with the results at the early and late stage of ECM.[25,30]

Cells can tolerate small changes in pH, but changes in pH comparable to the changes induced by PbA infection at the late stage of ECM are sufficient to affect cell function and normal neuronal activity function.[31] These changes in pH can activate ion channels and receptors, influencing brain function and behavior.[31] Reduced pH has been implicated in ischemic stroke, neurodegenerative disease, seizures, and respiratory dysfunction.[31] Subsequently, limited oxygenation and acidosis could be responsible for the neurological impairment during ECM. ECM mice showed hypothermia, which probably had an impact on blood flow and oxygenation, since hypothermia decreases blood flow in normal conditions.[32] On the other hand, the brain tissue under hypothermia decreases its metabolic rate.[33] Thus, it is unclear whether the hypothermia induced by ECM is the result of the pathological condition or a reflex response to preserve tissue viability. All the measured parameters except parasitemia and anemia were worse in C57BL/6 mice with ECM (and even worse in those with late-stage ECM) than in PbA-infected BALB/c mice at similar stage of infection. These ECM-resistant mice showed less severe tissue hypoxia, acidosis, and higher blood flow to wash out metabolic byproducts.

PbA-infected C57BL/6 mice with late-stage ECM were more anemic, underperfused, hypoxic, and acidotic than mice with early-stage ECM, although the number of adherent leukocytes in postcapillary venules was not different between these two subgroups. Vascular occlusion by adherent leukocytes, together with vasoconstriction,[18] increase vascular resistance[17] and are therefore major contributors for the impaired cerebral perfusion in ECM. It is likely that at a given threshold of impaired perfusion caused by vascular occlusion and vasoconstriction (with consequent hypoxia and acidosis), infected mice start to develop ECM signs (early-stage ECM), which rapidly evolve to become severe (late-stage ECM) without necessarily worsening the triggering events. Indeed, once mice show mild to moderate hypothermia they will rapidly evolve to a state of severe hypothermia. Studies have shown that $CD8^+$ T cells play an important role in the pathogenesis of ECM.[34,35] Depletion of $CD8^+$ T cells in mice with ECM preserves vascular damage and prevents death, as these cells damage the cerebral endothelium through release of perforin. In addition, the adherent $CD8^+$ T cells obstruct blood flow and impair perfusion, so the removal of the adherent $CD8^+$ T cells would have the additional benefit of improving cerebral blood flow and oxygenation. Nevertheless, the effect of $CD8^+$ T-cell depletion on brain oxygenation during ECM remains to be studied.

The findings of this study provide further confirmation that hypoperfusion resulting in ischemia and hypoxia is a key development in the pathogenesis of cerebral malaria. We have recently shown that, in addition to vascular occlusion, vasoconstriction is largely responsible for hypoperfusion in ECM,[18] and nitric oxide synthase dysfunction plays an important role in the associated vascular pathology.[36] In addition, continuous administration of the vasodilators nimodipine and glyceryl trinitrate improves cerebral perfusion and increases survival of mice with late-stage ECM.[18,37] These findings, together with the demonstration of cerebral hypoxia in this study, strongly indicate that interventions to restore cerebral perfusion, via restoring oxygenation and washing out metabolic waste, are of great benefit in the management of cerebral malaria in infected individuals. Clinically, erythropoietin (Epo) and hyperbaric oxygen therapy

have shown to reverse hypoxia in ECM and increase chance of survival.[38-41] High doses of Epo have been associated with protection from sequelae in children with cerebral malaria.[42] Hyperbaric oxygen therapy has also been shown to be of benefit in ECM.[41] However, clinical studies similar to the one conducted in this work are not feasible, as procedures such as retinal angiography indicate that hypoxia is also a key feature of human cerebral malaria.[6] Patients with cerebral malaria and mice with ECM exhibit a low central vascular resistance and elevated cardiac output.[37,43] Cardiac function appears remarkably well preserved despite intense sequestration of parasitized erythrocytes in the microvasculature of the myocardium. Therefore, interventions to treat cerebral malaria should aim to divert cardiac output to restore perfusion and to address the mechanisms that impair cerebral perfusion to reduce the risk of a fatal outcome in severe malaria cases.

Microvascular PO_2 measurements in the pial microcirculation have been generated before using microelectrodes.[44,45] In comparison to other techniques to investigate intravascular and perivascular PO_2s, PQM has fewer limitations compared with microelectrode measurements. Microelectrodes have to penetrate the vessel wall, where the tip exposes proteins and triggers thrombus formation, reducing blood flow and PO_2s. Microelectrode studies also include a superfusion solution that acts as a sink for O_2. PQM provides fast absolute measurements of PO_2, unaffected by tissue optical properties or dye concentration. PQM is limited by the photodamage and O_2 consumption from the quenching reaction (singlet O_2 and other reactive O_2 species), so PO_2 measurements were only performed at day 6 after infection (as our previous studies showed that cerebral blood flow in ECM occurs quite suddenly on day 6 after infection).[18] In addition, creating a time course of the changes in PO_2 would require an excessive amount of animals. Therefore, to prevent any effects in cell viability in our study, the Pd-porphyrin was administered only 10 min before PO_2 measurements. The blood brain barrier prevented excessive extravasation of the Pd-porphyrin albumin complex, thus perivascular emission intensities were 1/10 of intravascular emission intensities. To our surprise, the emission intensities did not increase in the early-state ECM group, even though ECM has been associated with breakdown of the blood brain barrier. The O_2 consumption of the PQM did not have an effect in our results, since no changes in lifetimes were observed when measurements were repeated at the same location.

In conclusion, this study provides for the first time a direct, quantitative and dynamic in vivo measurement of hypoxia in the different compartments (arterioles, perivascular tissue, and venules), revealing that low blood flow, anemia and low PO_2 levels cause marked decreases in O_2 delivery to the pial tisues. This study also shows the vulnerability of the pial tissue of mice with ECM to the changes in O_2 transport, as O_2 delivery and extraction occur within the steepest zone of the blood O_2 equilibrium curve. Thus, a minor decrease in blood flow or reduction in arteriolar PO_2 can drastically reduce O_2 delivery. On the other hand, ECM-resistant PbA-infected BALB/c mice seem to have a greater capacity to adapt to changes in flow and PO_2s compared with the ECM model. All these findings provide a more mechanistic

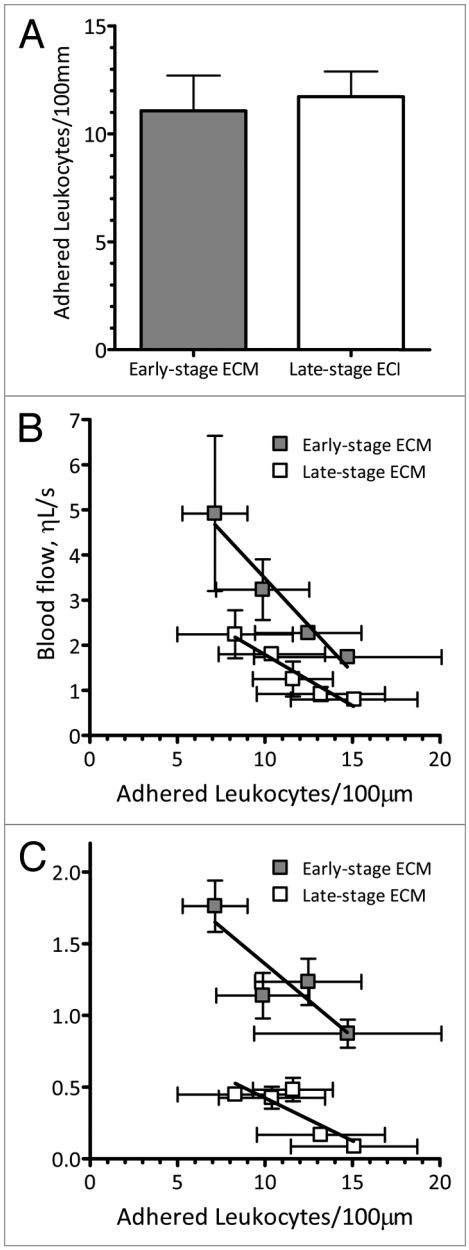

Figure 6. Adherent leukocytes relation to blood flow and O_2 extraction in PbA-infected animals with early- or late-stage ECM (C57BL/6). (**A**) Leukocyte adhesion with early- or late-stage ECM (C57BL/6) animals. (**B**) Leukocyte adhesion relationship to blood flow with early- or late-stage ECM (C57BL/6) animals. (**C**) Leukocyte adhesion relationship to O_2 extraction with early- or late-stage ECM (C57BL/6) animals. There was no difference in the leukocytes adhered to the endothelium between early- and late-stage ECM. There are overlapping ranges for leukocytes adhered and microvascular blood flow for both cohorts; thus blood flow in early- and late-stage ECM appears to be determined by the changes in vascular resistance produced the adhered leucocytes. Although the numbers of adhered leucocytes were not different for early- or late-stage ECM, O_2 extractions were different. Leukocyte adherence to the endothelium appears to be a factor decreasing blood flow, but no O_2 extraction.

understanding of cerebral hypoxia during PbA infection in ECM and non-ECM animals. Finally, this methodology will allow for directly studying the influence of interventions aimed to reverse or prevent hypoxia during malaria infection.

Materials and Methods

Closed cranial window animal preparation

Animal handling and care followed the NIH Guide for Care and Use of Laboratory Animals. All protocols were approved by the La Jolla Bioengineering Institutional Animal Care and Use Committee. Eight- to 10-week old C57Bl/6J and Balb/cJ mice (Jackson Laboratories) were implanted with a closed cranial window model as described elsewhere.[46] Briefly, mice were anesthetized with ketamine–xylazine and were administered dexamethasone (0.2 mg/kg), carprofen (5 mg/kg), and ampicillin (6 mg/kg) subcutaneously, in order to prevent postsurgical swelling of the brain, inflammatory response, and infection. After shaving the head and cleansing with ethanol 70% and betadine, the mouse was placed on a stereotaxic frame and the head immobilized using ear bars. The scalp was removed with sterilized surgical instruments and lidocaine–epinephrine was applied on the periosteum, which was then retracted to expose the skull. A 3–4 mm diameter skull opening was made in the left parietal bone using a surgical drill. Under a drop of saline, the craniotomy was lifted away from the skull with very thin-tip forceps and gelfoam previously soaked in saline was applied to the dura mater in order to stop any eventual small bleeding. The exposed area was covered with a 5 mm glass coverslip secured with cyanocrylate-based glue and dental acrylic. Carprofen and ampicillin were given daily for 3–5 d after recovery from surgery. Mice presenting signs of pain or discomfort were euthanized with 100 mg/kg of euthasol IP. Two to three weeks after surgery, mice fulfilling the inclusion criteria (see below) were inoculated with *P. berghei* ANKA and, on day 6 of infection, they were lightly anesthetized with isoflurane (4% for induction, 1–2% for maintenance) and held on a stereotaxic frame for measurements of pH and PO_2.

Inclusion criteria

Animals were suitable for the experiments if: (1) animal behavior was normal and (2) microscopic (350× magnification) examination of the cranial window did not reveal signs of edema or bleeding.

Parasite infection

Animals were inoculated with an IP injection of 1×10^6 *Plasmodium berghei* ANKA parasites expressing the green fluorescent protein (PbA-GFP, a donation from the Malaria Research and Reference Reagent Resource Center—MR4; deposited by CJ Janse and AP Waters; MR4 number: MRA-865). Parasitemia, body weight, rectal temperature, and clinical status (using 6 simple tests adapted from the SHIRPA protocol, as previously described) were monitored daily from day 4 of the infection.[47] Parasitemia was checked using flow cytometry by detecting the number of fluorescent GFP-expressing pRBCs in relation to 10 000 RBCs. ECM was diagnosed when one or more of the following clinical signs of neurological involvement were observed: ataxia, limb paralysis, poor righting reflex, seizures, roll-over, or coma.

Physiological ranges of the variables measured for the animal species used

Two groups of animals, C57BL/6 (n = 6) and BALB/c (n = 6), instrumented with the closed cranial window were used to characterize normal microhemodynamic (vessel diameter and blood flow), intravascular and perivascular PO_2s and pH in the pial microenvironment.

Experimental groups

Group 1 aimed to establish the effects of PbA infection in microhemodynamics, intravascular and perivascular PO_2s and pH in the pial microenvironment. The group consisted of ECM-susceptible C57BL/6 (infected, n = 14) and ECM-resistant BALB/c (infected, n = 9) mice. Uninfected C57BL/6 (n = 6) and BALB/c (n = 6) mice were included as controls. Control animals were manipulated in the exact same way as the infected mice (except for the infection itself). C57BL/6 ECM animals at day 6 of infection were divided in two cohorts: early-stage ECM, presenting mild to moderate drops in body temperature (>34 °C, <36 °C) and late-stage ECM, showing marked drops in body temperature (<33 °C). Another group, Group 2, was included to establish the relation between vascular inflammation resulting from PbA infection and microhemodynamics and oxygenation in relation to ECM pathophysiological changes. The group consisted of C57BL/6 (infected, n = 9) mice to which leukocyte adhesion, blood flow, and PO_2 levels were measured. Similarly as in Group 1, the ECM animals at day 6 of infection were divided in two cohorts: early-stage ECM and late-stage ECM. All experiments were repeated at least once.

Experimental setup

Animals were lightly anesthetized with isoflurane (4% for induction, 1–2% for maintenance). They were secured to the microscopic stage of an intravital microscope (BX51WI, Olympus) on a stereotaxic frame with the head gently held with ear bars for epi-illumination imaging. Body temperature, measured pre-anesthesia, was maintained with a heating pad. The tissue image was projected onto a charge-coupled device camera (COHU 4815) connected to a videocassette recorder and viewed on a monitor. Measurements were performed using a 40× (LUMPFL-WIR, numerical aperture 0.8, Olympus) water immersion objective. The animals did not recover from anesthesia, as they were euthanized (Euthasol 100 mg/kg, IP) right after the intravital microscopy measurements.

Microhemodynamics

A video image-shearing method was used to measure vessel diameter (D).[48] Changes in arteriolar and venular diameter from baseline were used as indicators of a change in vascular tone. Arteriolar and venular centerline velocities were measured online using the photodiode cross-correlation method (Photo Diode/Velocity Tracker Model 102B, Vista Electronics). The measured centerline velocity (V) was corrected according to vessel size to obtain the mean RBC velocity.[49] Blood flow (Q) was calculated from the measured values as $Q = \pi \times V \left(\frac{D}{2} \right)^2$.

This calculation assumes a parabolic velocity profile and has been found to be applicable to tubes of 15–80 μm internal diameters and for Hcts in the range of 6–60%.[49]

Microvascular PO_2 distribution

High resolution non-invasive microvascular PO_2 measurements were made using phosphorescence quenching microscopy (PQM).[50] PQM is based on the relationship between the decay rate of excited palladium-mesotetra-(4-carboxyphenyl) porphyrin (Frontier Scientific Porphyrin Products) bound to albumin and the O_2 concentration according to the Stern–Volmer equation.[50,51] The method was used previously in microcirculatory studies to determine PO_2 levels in different tissues.[51] PO_2 measurements by PQM were obtained following these steps for all groups: (1) the probe was injected (tail injection of 15 mg/kg at a concentration of 10 mg/ml of the phosphorescence complex 10 min before O_2 measurements); (2) the tissue was illuminated (pulsed light at 420 nm wavelength) to excite the probe into its triplet state; (3) the emitted phosphorescence (680 nm wavelength) was collected and analyzed to yield the phosphorescence lifetime; and (4) the phosphorescence lifetime was converted into O_2 concentration, PO_2. The phosphorescence lifetimes are concentration independent, which permit extravascular fluid PO_2 measurements, although the dye albumin complex that extravasates is very small. Extravascular fluid PO_2 was measured in regions in between functional capillaries. PQM allows for precise localization of the PO_2 measurements without subjecting the tissue to injury. These measurements provide a detailed understanding of microvascular O_2 distribution and indicate whether O_2 is delivered to the interstitial areas.

Perivascular pH measurement

Tail injection of 0.7 mg/kg of cell-impermeable fluorochrome 2′,7′-bis-(2-carboxyethyl)-5,6-carboxyfluorescein (BCECF; Molecular Probes) was given 15 min before measurements. Fluorescence emission signals (535 nm filter; Thorslabs Inc.) were recorded using a photomultiplier (R928; Hamamatsu) following 495 nm (pH-sensitive) and 440 nm (concentration-sensitive) light excitation (Thorslabs). The fluorescence ratio gives concentration-independent, pH measurements, $Emission_{535} = \frac{(I_{495} - I_{back\,495})}{(I_{440} - I_{back\,440})}$.[24] Background fluorescence intensities ($I_{back440}$ and $I_{back495}$) were recorded before dye injection and then subtracted from the corresponding fluorescence intensities. Fluorescence intensities were recorded for 5 s.

Endothelial leukocyte adhesion

The closed cranial window model was used as previously described.[18] On day 6 of PbA infection, anti-CD45-TxR antibodies (CalTag; 4 μg) were intravenously infused through the tail vein (volume: 50 μL). Using water-immersion objectives (20×), blood vessel images were captured using a CCD camera (COHU 4815). Fifteen minutes after injection red (615 nm) fluorescently labeled leukocytes were excited and images were captured with a Vivid Standard: XF42 filter. Adherence was defined as cells remaining static for 30 s. For each selected vessel, adherent leukocytes were quantified in a 100 μm length sections.

Hematocrit and hemoglobin

Blood was collected from the tail in heparinized glass capillaries. Hemoglobin was determined spectrophotometrically from a single drop of blood in a B-Hemoglobin analyzer (Hemocue). Hematocrit was estimated by centrifugation.

Blood oxygen equilibrium curve

Blood O_2 saturation curves were obtained by deoxygenation of O_2-equilibrated samples in a Hemox Analyzer (TCS Scientific Corporation) at animal's core body temperature and mean pial perivascular pH. The Hemox buffer pH was adjusted using Tris and BisTris buffers. Tris and BisTris buffers were prepared by titrating the reagents with HCI before adjusting the pH of the solutions to keep Cl^- ions concentration equal to the buffer at the pH values.

Oxygen delivery and extraction

The microvascular methodology used in our studies allows a detailed analysis of O_2 supply in the tissue. Calculations are made using Equations 1 and 2:

O_2 delivery: $DO_2 = RBC_{Hb} \times \gamma \times S_A \times Q_A$ (1)

$O_{2\,A\text{-}V}$ extraction: $VO_2 = RBC_{Hb} \times \gamma \times S_{A-V} \times Q_{A-V}$ (2)

Where RBC_{Hb} is the total Hb [g_{Hb/dL_blood}], γ is the O_2 carrying capacity of saturated hemoglobin [1.34 mlO_2/g_{Hb}], S_A is the arteriolar blood O_2 saturation, SA-V indicates the arteriolar/venular saturation differences, Q_A is arteriolar microvascular flow and $Q_{A\text{-}V}$ is average of arteriolar/venular microvascular flows. O_2 extraction radio was calculated as the ratio of O_2 delivery to $O_{2\,A\text{-}V}$ extraction. O_2 saturations were calculated using blood O_2 equilibrium curve.

Data analysis

Results are presented as mean ± standard deviation, except for vessel diameters and blood flows, which are presented as box-whisker plots. Microhemodynamics and PO_2 data are presented as absolute values. Data between groups was analyzed by an analysis of variance (ANOVA, Kruskal–Wallis test). When appropriate, post hoc analyses were performed with the Dunns multiple comparison test. Spearmen correlation coefficient gives an *R* estimate and is a measure of monotone association that is used when the distribution of the data make Pearson correlation coefficient undesirable or misleading. All statistics were calculated using GraphPad Prism 4.01 (GraphPad Software, Inc.). Changes were considered statistically significant if $P < 0.05$.

Disclosure of Potential Conflicts of Interest

The authors declare that there are no conflicts of interest.

Financial Disclosure

The funders had no role in study design, data collection and analysis, decision to publish, or preparation of the manuscript.

Acknowledgments

This work was supported by grants R01-AI82610, R01-HL52684, and MERIT R37-HL040696.

References

1. Idro R, Jenkins NE, Newton CR. Pathogenesis, clinical features, and neurological outcome of cerebral malaria. Lancet Neurol 2005; 4:827-40; PMID:16297841; http://dx.doi.org/10.1016/S1474-4422(05)70247-7
2. Idro R. Severe anaemia in childhood cerebral malaria is associated with profound coma. Afr Health Sci 2003; 3:15-8; PMID:12789083
3. Maitland K, Marsh K. Pathophysiology of severe malaria in children. Acta Trop 2004; 90:131-40; PMID:15177139; http://dx.doi.org/10.1016/j.actatropica.2003.11.010
4. von Seidlein L, Olaosebikan R, Hendriksen IC, Lee SJ, Adedoyin OT, Agbenyega T, Nguah SB, Bojang K, Deen JL, Evans J, et al. Predicting the clinical outcome of severe falciparum malaria in african children: findings from a large randomized trial. Clin Infect Dis 2012; 54:1080-90; PMID:22412067; http://dx.doi.org/10.1093/cid/cis034
5. Rénia L, Wu Howland S, Claser C, Charlotte Gruner A, Suwanarusk R, Hui Teo T, Russell B, Ng LF. Cerebral malaria: mysteries at the blood-brain barrier. Virulence 2012; 3:193-201; PMID:22460644; http://dx.doi.org/10.4161/viru.19013
6. Beare NA, Harding SP, Taylor TE, Lewallen S, Molyneux ME. Perfusion abnormalities in children with cerebral malaria and malarial retinopathy. J Infect Dis 2009; 199:263-71; PMID:18999956; http://dx.doi.org/10.1086/595735
7. Pongponratn E, Riganti M, Punpoowong B, Aikawa M. Microvascular sequestration of parasitized erythrocytes in human falciparum malaria: a pathological study. Am J Trop Med Hyg 1991; 44:168-75; PMID:2012260
8. John CC, Bangirana P, Byarugaba J, Opoka RO, Idro R, Jurek AM, Wu B, Boivin MJ. Cerebral malaria in children is associated with long-term cognitive impairment. Pediatrics 2008; 122:e92-9; PMID:18541616; http://dx.doi.org/10.1542/peds.2007-3709
9. White NJ, Warrell DA, Looareesuwan S, Chanthavanich P, Phillips RE, Pongpaew P. Pathophysiological and prognostic significance of cerebrospinal-fluid lactate in cerebral malaria. Lancet 1985; 1:776-8; PMID:2858665; http://dx.doi.org/10.1016/S0140-6736(85)91445-X
10. MacPherson GG, Warrell MJ, White NJ, Looareesuwan S, Warrell DA. Human cerebral malaria. A quantitative ultrastructural analysis of parasitized erythrocyte sequestration. Am J Pathol 1985; 119:385-401; PMID:3893148
11. Beare NA, Glover SJ, Molyneux M. Malarial retinopathy in cerebral malaria. Am J Trop Med Hyg 2009; 80:171; PMID:19190205
12. Sanni LA, Rae C, Maitland A, Stocker R, Hunt NH. Is ischemia involved in the pathogenesis of murine cerebral malaria? Am J Pathol 2001; 159:1105-12; PMID:11549603; http://dx.doi.org/10.1016/S0002-9440(10)61786-5
13. Rae C, McQuillan JA, Parekh SB, Bubb WA, Weiser S, Balcar VJ, Hansen AM, Ball HJ, Hunt NH. Brain gene expression, metabolism, and bioenergetics: interrelationships in murine models of cerebral and noncerebral malaria. FASEB J 2004; 18:499-510; PMID:15003995; http://dx.doi.org/10.1096/fj.03-0543com
14. Hempel C, Combes V, Hunt NH, Kurtzhals JA, Grau GE. CNS hypoxia is more pronounced in murine cerebral than noncerebral malaria and is reversed by erythropoietin. Am J Pathol 2011; 179:1939-50; PMID:21854739; http://dx.doi.org/10.1016/j.ajpath.2011.06.027
15. Tripathy R, Parida S, Das L, Mishra DP, Tripathy D, Das MC, Chen H, Maguire JH, Panigrahi P. Clinical manifestations and predictors of severe malaria in Indian children. Pediatrics 2007; 120:e454-60; PMID:17766489; http://dx.doi.org/10.1542/peds.2006-3171
16. Cabrales P, Carvalho LJ. Intravital microscopy of the mouse brain microcirculation using a closed cranial window. J Vis Exp 2010; PMID:21113121; http://dx.doi.org/10.3791/2184
17. Zanini GM, Cabrales P, Barkho W, Frangos JA, Carvalho LJ. Exogenous nitric oxide decreases brain vascular inflammation, leakage and venular resistance during Plasmodium berghei ANKA infection in mice. J Neuroinflammation 2011; 8:66; PMID:21649904; http://dx.doi.org/10.1186/1742-2094-8-66
18. Cabrales P, Zanini GM, Meays D, Frangos JA, Carvalho LJ. Murine cerebral malaria is associated with a vasospasm-like microcirculatory dysfunction, and survival upon rescue treatment is markedly increased by nimodipine. Am J Pathol 2010; 176:1306-15; PMID:20110412; http://dx.doi.org/10.2353/ajpath.2010.090691
19. Cabrales P, Zanini GM, Meays D, Frangos JA, Carvalho LJ. Nitric oxide protection against murine cerebral malaria is associated with improved cerebral microcirculatory physiology. J Infect Dis 2011; 203:1454-63; PMID:21415018; http://dx.doi.org/10.1093/infdis/jir058
20. Abbott NJ. Inflammatory mediators and modulation of blood-brain barrier permeability. Cell Mol Neurobiol 2000; 20:131-47; PMID:10696506; http://dx.doi.org/10.1023/A:1007074420772
21. Zhao F, Wang P, Kim SG. Cortical depth-dependent gradient-echo and spin-echo BOLD fMRI at 9.4T. Magn Reson Med 2004; 51:518-24; PMID:15004793; http://dx.doi.org/10.1002/mrm.10720
22. Delahaye NF, Coltel N, Puthier D, Flori L, Houlgatte R, Iraqi FA, Nguyen C, Grau GE, Rihet P. Gene-expression profiling discriminates between cerebral malaria (CM)-susceptible mice and CM-resistant mice. J Infect Dis 2006; 193:312-21; PMID:16362897; http://dx.doi.org/10.1086/498579
23. Helegbe GK, Yanagi T, Senba M, Huy NT, Shuaibu MN, Yamazaki A, Kikuchi M, Yasunami M, Hirayama K. Histopathological studies in two strains of semi-immune mice infected with Plasmodium berghei ANKA after chronic exposure. Parasitol Res 2011; 108:807-14; PMID:20978790; http://dx.doi.org/10.1007/s00436-010-2121-6
24. Cabrales P, Nacharaju P, Manjula BN, Tsai AG, Acharya SA, Intaglietta M. Early difference in tissue pH and microvascular hemodynamics in hemorrhagic shock resuscitation using polyethylene glycol-albumin- and hydroxyethyl starch-based plasma expanders. Shock 2005; 24:66-73; PMID:15988323; http://dx.doi.org/10.1097/01.shk.0000167111.80753.ef
25. van Santbrink H, Maas AI, Avezaat CJ. Continuous monitoring of partial pressure of brain tissue oxygen in patients with severe head injury. Neurosurgery 1996; 38:21-31; PMID:8747947; http://dx.doi.org/10.1097/00006123-199601000-00007
26. Schmidt W, Correa R, Böning D, Ehrich JH, Krüger C. Oxygen transport properties in malaria-infected rodents--a comparison between infected and noninfected erythrocytes. Blood 1994; 83:3746-52; PMID:8204895
27. Paulson OB, Hasselbalch SG, Rostrup E, Knudsen GM, Pelligrino D. Cerebral blood flow response to functional activation. J Cereb Blood Flow Metab 2010; 30:2-14; PMID:19738630; http://dx.doi.org/10.1038/jcbfm.2009.188
28. Warrell DA, White NJ, Veall N, Looareesuwan S, Chanthavanich P, Phillips RE, Karbwang J, Pongpaew P, Krishna S. Cerebral anaerobic glycolysis and reduced cerebral oxygen transport in human cerebral malaria. Lancet 1988; 2:534-8; PMID:2900921; http://dx.doi.org/10.1016/S0140-6736(88)92658-X
29. Jóhannsson H, Siesjö BK. Blood flow and oxygen consumption in the rat brain in dilutional anemia. Acta Physiol Scand 1974; 91:136-8; PMID:4835719; http://dx.doi.org/10.1111/j.1748-1716.1974.tb05667.x
30. Cruz J, Jaggi JL, Hoffstad OJ. Cerebral blood flow and oxygen consumption in acute brain injury with acute anemia: an alternative for the cerebral metabolic rate of oxygen consumption? Crit Care Med 1993; 21:1218-24; PMID:8339590; http://dx.doi.org/10.1097/00003246-199308000-00024
31. Magnotta VA, Heo HY, Dlouhy BJ, Dahdaleh NS, Follmer RL, Thedens DR, Welsh MJ, Wemmie JA. Detecting activity-evoked pH changes in human brain. Proc Natl Acad Sci U S A 2012; 109:8270-3; PMID:22566645; http://dx.doi.org/10.1073/pnas.1205902109
32. Gur RC, Ragland JD, Reivich M, Greenberg JH, Alavi A, Gur RE. Regional differences in the coupling between resting cerebral blood flow and metabolism may indicate action preparedness as a default state. Cereb Cortex 2009; 19:375-82; PMID:18534991; http://dx.doi.org/10.1093/cercor/bhn087
33. Zhu X-H, Chen J, Tu T-W, Chen W, Song S-K. Simultaneous and noninvasive imaging of cerebral oxygen metabolic rate, blood flow and oxygen extraction fraction in stroke mice. Neuroimage 2013; PMID:23000789
34. Randall LM, Amante FH, McSweeney KA, Zhou Y, Stanley AC, Haque A, Jones MK, Hill GR, Boyle GM, Engwerda CR. Common strategies to prevent and modulate experimental cerebral malaria in mouse strains with different susceptibilities. Infect Immun 2008; 76:3312-20; PMID:18474652; http://dx.doi.org/10.1128/IAI.01475-07
35. Belnoue E, Kayibanda M, Vigario AM, Deschemin JC, van Rooijen N, Viguier M, Snounou G, Rénia L. On the pathogenic role of brain-sequestered alphabeta CD8+ T cells in experimental cerebral malaria. J Immunol 2002; 169:6369-75; PMID:12444144
36. Ong PK, Melchior B, Martins YC, Hofer A, Orjuela-Sánchez P, Cabrales P, Zanini GM, Frangos JA, Carvalho LJ. Nitric oxide synthase dysfunction contributes to impaired cerebroarteriolar reactivity in experimental cerebral malaria. PLoS Pathog 2013; 9:e1003444; PMID:23818850; http://dx.doi.org/10.1371/journal.ppat.1003444
37. Martins YC, Clemmer L, Orjuela-Sánchez P, Zanini GM, Ong PK, Frangos JA, Carvalho LJ. Slow and continuous delivery of a low dose of nimodipine improves survival and electrocardiogram parameters in rescue therapy of mice with experimental cerebral malaria. Malar J 2013; 12:138; PMID:23617605; http://dx.doi.org/10.1186/1475-2875-12-138
38. Hempel C, Combes V, Hunt NH, Kurtzhals JAL, Grau GER. CNS hypoxia is more pronounced in murine cerebral than noncerebral malaria and is reversed by erythropoietin. Am J Pathol 2011; 179:1939-50; PMID:21854739; http://dx.doi.org/10.1016/j.ajpath.2011.06.027
39. Wiese L, Hempel C, Penkowa M, Kirkby N, Kurtzhals JA. Recombinant human erythropoietin increases survival and reduces neuronal apoptosis in a murine model of cerebral malaria. Malar J 2008; 7:3; PMID:18179698; http://dx.doi.org/10.1186/1475-2875-7-3
40. Bienvenu AL, Picot S. Cerebral malaria: protection by erythropoietin. Methods Mol Biol 2013; 982:315-24; PMID:23456877; http://dx.doi.org/10.1007/978-1-62703-308-4_19

41. Blanco YC, Farias AS, Goelnitz U, Lopes SC, Arrais-Silva WW, Carvalho BO, Amino R, Wunderlich G, Santos LM, Giorgio S, et al. Hyperbaric oxygen prevents early death caused by experimental cerebral malaria. PLoS One 2008; 3:e3126; PMID:18769544; http://dx.doi.org/10.1371/journal.pone.0003126
42. Casals-Pascual C, Idro R, Gicheru N, Gwer S, Kitsao B, Gitau E, Mwakesi R, Roberts DJ, Newton CR. High levels of erythropoietin are associated with protection against neurological sequelae in African children with cerebral malaria. Proc Natl Acad Sci U S A 2008; 105:2634-9; PMID:18263734; http://dx.doi.org/10.1073/pnas.0709715105
43. Trampuz A, Jereb M, Muzlovic I, Prabhu RM. Clinical review: Severe malaria. Crit Care 2003; 7:315-23; PMID:12930555; http://dx.doi.org/10.1186/cc2183
44. Vovenko EP, Chuikin AE. Oxygen tension in rat cerebral cortex microvessels in acute anemia. Neurosci Behav Physiol 2008; 38:493-500; PMID:18607751; http://dx.doi.org/10.1007/s11055-008-9007-4
45. Vovenko EP, Chuikin AE. Tissue oxygen tension profiles close to brain arterioles and venules in the rat cerebral cortex during the development of acute anemia. Neurosci Behav Physiol 2010; 40:723-31; PMID:20635218; http://dx.doi.org/10.1007/s11055-010-9318-0
46. Mostany R, Portera-Cailliau C. A craniotomy surgery procedure for chronic brain imaging. J Vis Exp 2008; PMID:19066562; http://dx.doi.org/10.3791/680
47. Lackner P, Beer R, Heussler V, Goebel G, Rudzki D, Helbok R, Tannich E, Schmutzhard E. Behavioural and histopathological alterations in mice with cerebral malaria. Neuropathol Appl Neurobiol 2006; 32:177-88; PMID:16599946; http://dx.doi.org/10.1111/j.1365-2990.2006.00706.x
48. Intaglietta M, Tompkins WR. Microvascular measurements by video image shearing and splitting. Microvasc Res 1973; 5:309-12; PMID:4709728; http://dx.doi.org/10.1016/0026-2862(73)90042-3
49. Lipowsky HH, Zweifach BW. Application of the "two-slit" photometric technique to the measurement of microvascular volumetric flow rates. Microvasc Res 1978; 15:93-101; PMID:634160; http://dx.doi.org/10.1016/0026-2862(78)90009-2
50. Torres Filho IP, Terner J, Pittman RN, Proffitt E, Ward KR. Measurement of hemoglobin oxygen saturation using Raman microspectroscopy and 532-nm excitation. J Appl Physiol 2008; 104:1809-17; PMID:18369097; http://dx.doi.org/10.1152/japplphysiol.00025.2008
51. Kerger H, Groth G, Kalenka A, Vajkoczy P, Tsai AG, Intaglietta M. pO(2) measurements by phosphorescence quenching: characteristics and applications of an automated system. Microvasc Res 2003; 65:32-8; PMID:12535869; http://dx.doi.org/10.1016/S0026-2862(02)00027-4